

LEARNED COMPLEX MASKS FOR MULTI-INSTRUMENT SOURCE SEPARATION

Andreas Jansson², Rachel M. Bittner¹, Nicola Montecchio¹, Tillman Weyde²

¹ Spotify, ² City University of London

ABSTRACT

Music source separation in the time-frequency domain is commonly achieved by applying a soft or binary mask to the magnitude component of (complex) spectrograms. The phase component is usually not estimated, but instead copied from the mixture and applied to the magnitudes of the estimated isolated sources. While this method has several practical advantages, it imposes an upper bound on the performance of the system, where the estimated isolated sources inherently exhibit audible “phase artifacts”. In this paper we address these shortcomings by directly estimating masks in the complex domain, extending recent work from the speech enhancement literature. The method is particularly well suited for multi-instrument musical source separation since residual phase artifacts are more pronounced for spectrally overlapping instrument sources, a common scenario in music. We show that complex masks result in better separation than masks that operate solely on the magnitude component.

Index Terms— source separation, music, complex mask

1. INTRODUCTION

Musical audio mixtures can be modeled as a sum of individual sources, and musical audio source separation aims to estimate these individual sources given the mixture. A common way to frame this problem is to separate a music recording into percussion, bass, guitar, voice, and “other” signals. *Spectral masking* is a common technique used in this context: a “mask” of the signal’s spectrogram is estimated, whose aim is to selectively “let through” only the components of the input signal corresponding to the particular source [1].

Typically, masks (both binary and soft) are only applied to the magnitude component of the input (complex) spectrogram, and the phase from the mixture is reused for each of the sources. This results in significant phase artifacts: sources that overlap in time and frequency with the target source leave audible traces in the masked signal. This effect is more pronounced the greater the spectral overlap between sources is, and is especially problematic in the music domain: due to the very nature of music, musical instruments and voices are often synchronous in time by following a shared meter (unlike speech), and their spectral components tend to occupy the same frequency ranges.

In this paper we present an approach that uses *complex-valued* masks as a drop-in replacement for magnitude-domain masks.

2. RELATED WORK

Neural network-based approaches have been applied to the problem of audio source separation for over a decade. For a review of such techniques in the speech domain, see [2].

In the music domain, the majority of Neural network-based models operates on time-frequency representations (spectrograms) of both the input and output signals; usually separation is achieved using masks in the magnitude domain. Different network architectures – both convolutional [3, 4] and recurrent [5] – have been used to separate vocals from accompaniment, as well as for multi-instrument separation. Skip connections, introduced in [6], have emerged as a common feature of source separation networks, because of their ability to carry fine-grained details from the input mixture representation to the layers closer to the final output representation. The U-Net [7] is a relatively simple application of skip connections: an hourglass-shaped convolutional encoder-decoder pair is augmented with connections between earlier layers of the encoder to later layers in the decoder. U-Nets have been applied to musical source separation in [4, 8].

A number of recent systems propose alternative models that avoid dealing with phase information altogether, by operating directly in the time domain: in [9], the authors construct a non-causal WaveNet [10] for speech enhancement entirely in the time domain; Wave-U-Net [11] is an extension of WaveNet that adds skip connections in the time domain, analogous to the U-Net in the frequency domain.

Other approaches attempt to explicitly make use of phase in the time-frequency domain: in [12] incorporating phase information in the mask function results in more accurate source estimation, even though the mask itself is real-valued. Predicting phase directly appears to be intractable [13], presumably because of the lack of inherent structure due to the wrap-around nature of phase; proposed solutions make use of *phase unwrapping* [14, 15] or discretization of phase [16].

In the speech domain, the complex Ideal Ratio Mask (cIRM) was introduced in [13] as the real and imaginary ratios between complex source and mixture spectrograms.

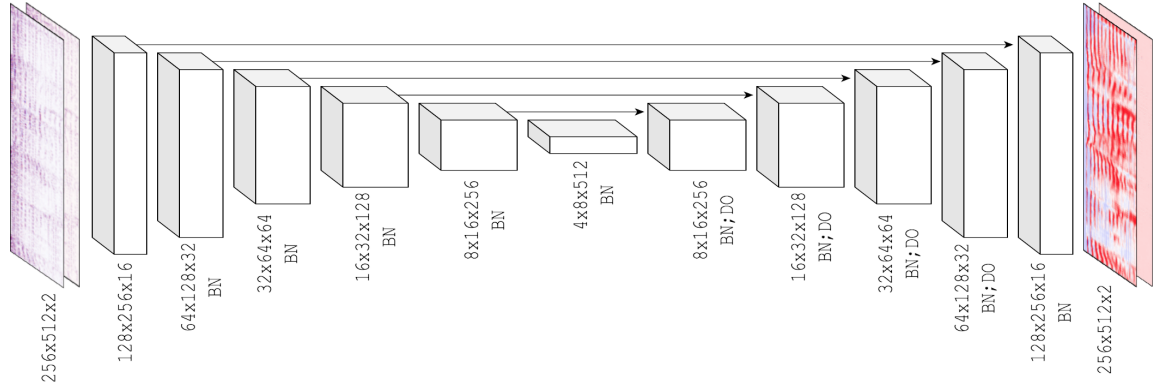


Fig. 1: Architecture diagram of the proposed model.

The Phase-U-Net [17] estimates complex masks, either using a real-valued internal representation or introducing the complex-valued equivalent of the traditional neural network building blocks such as matrix multiplication and convolution; the paper also deals with masking using a complex representation based on polar coordinates, and constraining the magnitude component.

Typically, methods based on a time-frequency representation are trained using a loss function which measures the distance (in L1 or L2 norm) between a target spectrogram (coming from an individually-recorded instrument, subsequently mixed to create the input signal) and the input spectrogram after the application of the predicted mask. More sophisticated designs allow a more direct optimization of evaluation measures, such as source-to-distortion ratio (SDR) [18, 17].

3. MODEL

3.1. Datasets

The proposed model is trained on a dataset of about 2000 professional-quality recordings. For each recording, five *stems* are available, grouped by instrument: “Vocals”, “Guitar”, “Bass”, “Percussion”, and “Other”. Each recording is, by design, the (unweighted) sum of its five stems.

To increase the size of the training set, a series of augmentation steps is performed on the stems. The augmentations include global, track-level changes – such as a time stretching, pitch shifting, or resampling – applied across all stems, and individual, stem-level changes, such as volume adjustments, equalization/filtering, effects such as phasers and flangers, and reverb. For each example in the training set, 10 random augmentations are generated.

For validation and testing, the MUSDB 2018 dataset [19] is used. MUSDB contains only 4 instrument types, namely “Vocals”, “Bass”, “Percussion”, and “Other”. When running validation and test results, we group our model’s outputs for “Guitar” into the “Other” category.

3.2. Architecture

The proposed model extends the U-Net source separation model detailed in [4], which in turn extends [20]; pictured in Figure 1, it consists of 6 downsampling “encoder” layers, 6 upsampling “decoder” layers, and skip connections between corresponding encoder and decoder layers. The network operates on spectrograms extracted from 22050 Hz mono audio signals, with overlapping windows of size 1024, and hop size 256. Each encoder layer comprises a strided convolution (with kernel size 5×5 and stride 2×2) followed by batch normalization (except in the first layer), and a leaky ReLU activation function. In the decoder, each layer consists of a strided transpose convolution (with kernel size 5×5 and stride 2×2 , as in the encoder); batch normalization is applied to all decoder layers except the last, as well as 50% dropout in the first five layers, and a ReLU activation function in all layers except the last.

3.3. Input and Output Representation

For multi-source separation, independent models are trained for vocals, drums, guitar, and bass. The “Other” source is estimated as the residual difference between mixture and the sum of the four estimated sources. Each source-specific network is presented with mixture spectrograms, which during training are sliced into patches of 256 frames, and fed in batches of 16 patches. This is not necessary during inference, since the network is fully convolutional and can be applied to the spectrogram of the full length of the signal.

The network is trained to output a mask that is then applied to the mixture spectrogram to produce the source spectrogram estimate. We evaluate two variations of this architecture: non-complex, where the input is a single mono channel representing the magnitude of the mixture spectrogram; and complex, where the input is the complex spectrogram, represented as independent real and imaginary channels. In the non-complex case, the mask is only applied to the magnitude component of the mixture, whereas in the complex case the

mask is applied in the complex domain. After mask application, we synthesize the estimated source signal by means of the Inverse Short-Time Fourier Transform (ISTFT).

It should be noted that in the complex case, although the input and output representations are both complex, the network itself is internally real-valued.

3.4. Masking

In the remainder of this section, $\mathbf{O}^{\mathbb{C}}$ and $\mathbf{O}^{\mathbb{R}}$ denotes the outputs by the complex and non-complex networks; $\mathbf{M}^{\mathbb{C}}$ and $\mathbf{M}^{\mathbb{R}}$ denotes complex and non-complex masks; \mathbf{X} denotes the spectrogram of the input mixture to be separated by the model; for individual stems (individual instruments or voice), \mathbf{Y} and $\hat{\mathbf{Y}}$ denote the spectrograms of the recorded and estimated stems, respectively, while \mathbf{y} and $\hat{\mathbf{y}}$ denote their time-domain equivalents.

3.4.1. Non-complex masking

The non-complex mask is computed as $\mathbf{M}^{\mathbb{R}} = \sigma(\mathbf{O}^{\mathbb{R}})$ where σ is the sigmoid function, constraining the (real-valued) network output to the (0,1) range. It is multiplied element-wise (denoted by \otimes) with the mixture spectrogram magnitude to obtain the estimated source spectrogram magnitude. The phase is copied from the mixture spectrogram into the spectrogram of the estimated stem, unaltered.

$$\hat{\mathbf{Y}} = \mathbf{M}^{\mathbb{R}} \otimes |\mathbf{X}| \otimes e^{i\angle\mathbf{X}} \quad (1)$$

3.4.2. Complex masking

In the complex case we estimate a complex-domain mask as in [17], constrained in magnitude but not in phase:

$$|\mathbf{M}^{\mathbb{C}}| = \tanh(|\mathbf{O}^{\mathbb{C}}|) \quad (2)$$

$$\angle\mathbf{M}^{\mathbb{C}} = \mathbf{O}^{\mathbb{C}} \oslash |\mathbf{O}^{\mathbb{C}}| \quad (3)$$

where \oslash denotes element-wise division. The complex mask is then applied element-wise, as:

$$\hat{\mathbf{Y}} = |\mathbf{M}^{\mathbb{C}}| \otimes |\mathbf{X}| \otimes e^{i(\angle\mathbf{M}^{\mathbb{C}} + \angle\mathbf{X})} \quad (4)$$

The mask applied determines a magnitude rescaling of the mixture STFT and a rotation (addition) in phase. This allows the model not only to remove interfering frequency bins, but also to cancel the phase from other sources.

3.5. Loss

We evaluate three different loss functions: *Magnitude loss*, *SDR loss*, and the combination *SDR + Magnitude loss*.

The *Magnitude loss* is optimized by minimizing the L1 distance between the spectrogram magnitudes of the estimated and target components:

$$\mathcal{L}_{\text{Mag}} = \|\mathbf{Y} - \hat{\mathbf{Y}}\|_1 \quad (5)$$

The time-domain *SDR loss* [17] is defined as:

$$\mathcal{L}_{\text{SDR}} = -\frac{\mathbf{y} \cdot \hat{\mathbf{y}}}{\|\mathbf{y}\| \|\hat{\mathbf{y}}\|} \quad (6)$$

which smoothly upper bounds the SDR metric we are interested in optimizing.

The hybrid time-domain and frequency-domain *SDR + Magnitude loss* is defined as:

$$\mathcal{L}_{\text{SDR+Mag}} = \mathcal{L}_{\text{SDR}} + \mathcal{L}_{\text{Mag}} \quad (7)$$

4. RESULTS

Two configurations of the system (“Non-complex”, “Complex-SDR”) are evaluated on the MUSDB 18 dataset, using the *museval* toolkit [21]; results are shown in Figure 3.

There are slight differences between the results of the different models when considering different metrics, however the complex model achieves higher Signal to Distortion Ratio (commonly considered the most important metric) than the non-complex model for most sources. Although these results do not compare favorably to State-of-the-Art approaches, such as those reported in the yearly SiSEC evaluation campaign [21], they do yield insights into the design of such systems, by providing a unified comparison not only in terms of dataset, but also through the use of a single model in which individual aspects (masking, loss function) are controlled.

We also collected subjective judgments from a number of individuals, using a methodology similar to that of [22]. A questionnaire was prepared, in which subjects were prompted to compare audio recordings in pairs, each pair presenting the outputs of two different model configurations applied the same short audio excerpt. As a reference, evaluators were given both the original mixture and the target single source signal.

Two questions were asked per pair of audio excerpts: “Quality: Which one has better sound quality?”, and “Separation: Which one has better isolation from the other instruments in the original mix?”. We collected 210 judgements from 8 individuals trained in audio engineering.

We found that in 58% of the “Separation” questions, SDR loss was preferred to non-complex loss. The effect was stronger for the “Quality” question, where 65% of judgments preferred SDR loss. The preference for SDR loss was most pronounced on bass, followed by percussion and vocals.

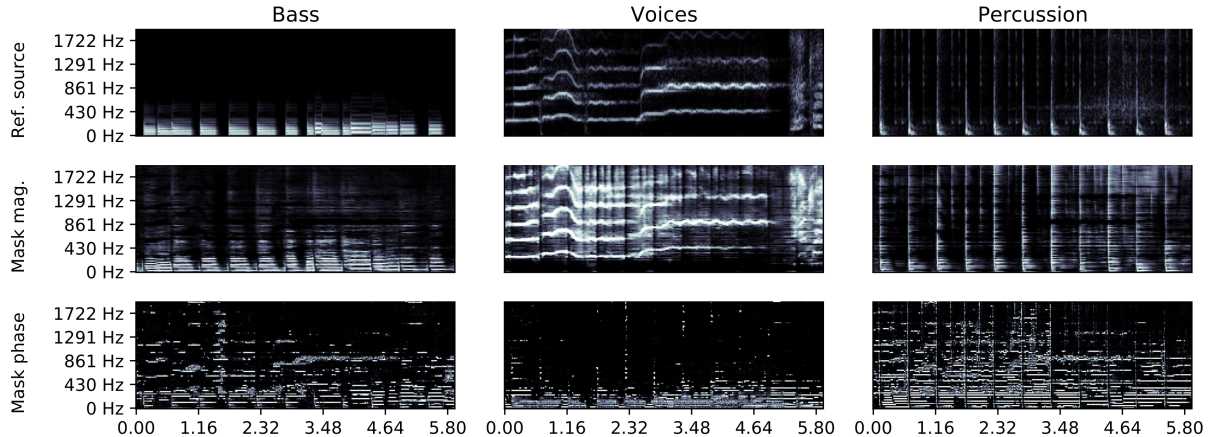


Fig. 2: Magnitude and phase of learned complex masks (Complex-SDR) for Bass, Voices, and Percussion on a test example from MUSDB18, and the reference STFTs for each source. **Top Row:** Magnitude (dB) of the ideal STFTs. **Middle Row:** Magnitude of the learned complex masks. **Bottom Row:** Absolute value of the phase of the learned complex masks.

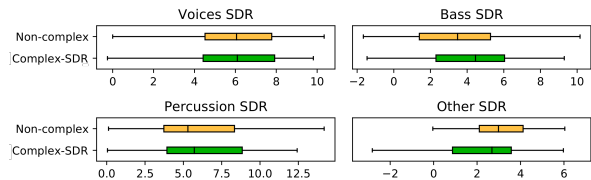


Fig. 3: Signal to Distortion Ratio across experiments.

4.1. Qualitative Analysis

A website with audio examples of the complex and non-complex masks can be found online ¹. The biggest audible difference between the audio output by the complex masking model and the non-complex masking model is the amount of phase distortion, in particular for bass and percussion. When using real masks, both bass and percussion tend to sound very tinny, and the phase of other sources is often captured in the sound of the reconstructed source, such as hearing faint voices in a percussion signal. The predicted vocals sound similar in both models, and the overall quality is rather good.

4.2. Analysis of learned masks

Figure 2 displays the learned masks from the Complex-SDR model on a recording, and the STFTs of the clean reference sources; the middle and bottom rows show the magnitude and (absolute) phase of the learned masks respectively. As expected, the magnitude of the learned masks looks like that of a typical soft mask, where the time frequency bins of the target source have values close to 1 and other bins have values close to 0. For bass, harmonic patterns with few transients in the low frequency range are noticeable; for voice, harmonic patterns tend to inhabit a higher frequency range and exhibit

stronger transients, e.g., at the starts of words; percussion exhibits more regular transients.

The phase of the mask determines how much the phase of the mixture should be rotated: higher values indicate places where the phase of the mixture is substantially different from the phase of the source (e.g., because it overlaps with another source). In this example, we see that for percussion there are large phase corrections being made for horizontal patterns, likely canceling the phase from harmonic sources in the mixture. Additionally, the phase is corrected the instant before an onset, which makes the onset sound more crisp than if it were smeared with phase from other sources. For the vocal signal, most of the phase corrections are made where the bass and percussion masks are active, indicating that the phase of the bass and percussion is being canceled out for the vocal mask. Close inspection of the phase of the bass mask reveals that lower frequency bands that have large values from the mask and for the phase are interleaved, implying that the phase of closely overlapping low frequency sources is being canceled.

5. CONCLUSIONS

The use of complex masks for multi-instrument source separation is explored using a U-Net architecture. It was found that learned complex masks perform better than non-complex masks perceptually, and marginally better in terms of SDR. Analysis of the learned masks highlights a particularly strong effect on percussion and bass. As a result, the constrained complex mask is a practical, low effort, drop-in replacement for common magnitude-domain masks.

6. REFERENCES

- [1] DeLiang Wang, “On ideal binary mask as the computational goal of auditory scene analysis,” in *Speech separation*

¹<http://bit.ly/lcmmiss>

- ration by humans and machines, pp. 181–197. Springer, 2005.
- [2] DeLiang Wang and Jitong Chen, “Supervised speech separation based on deep learning: An overview,” *IEEE/ACM Trans. Audio, Speech & Language Processing*, vol. 26, no. 10, pp. 1702–1726, 2018.
 - [3] Andrew JR Simpson, Gerard Roma, and Mark D Plumbley, “Deep karaoke: Extracting vocals from musical mixtures using a convolutional deep neural network,” in *Latent Variable Analysis and Signal Separation*, Emmanuel Vincent, Arie Yeredor, Zbyněk Koldovský, and Petr Tichavský, Eds. 8 2015, Lecture Notes in Computer Science, pp. 429–436, Springer, Cham.
 - [4] A Jansson, E Humphrey, N Montecchio, R Bittner, A Kumar, and T Weyde, “Singing voice separation with deep u-net convolutional networks,” in *18th International Society for Music Information Retrieval Conference*, 2017, pp. 23–27.
 - [5] Po-Sen Huang, Minje Kim, Mark Hasegawa-Johnson, and Paris Smaragdis, “Deep learning for monaural speech separation,” in *ICASSP*. 2014, pp. 1562–1566, IEEE.
 - [6] Kaiming He, Xiangyu Zhang, Shaoqing Ren, and Jian Sun, “Deep residual learning for image recognition,” in *Proceedings of the IEEE conference on computer vision and pattern recognition*, 2016, pp. 770–778.
 - [7] Olaf Ronneberger, Philipp Fischer, and Thomas Brox, “U-net: Convolutional networks for biomedical image segmentation,” in *International Conference on Medical image computing and computer-assisted intervention*. Springer, 2015, pp. 234–241.
 - [8] Sungheon Park, Taehoon Kim, Kyogu Lee, and Nojun Kwak, “Music source separation using stacked hourglass networks,” in *ISMIR*, Emilia Gómez, Xiao Hu, Eric Humphrey, and Emmanouil Benetos, Eds., 2018, pp. 289–296.
 - [9] Dario Rethage, Jordi Pons, and Xavier Serra, “A wavenet for speech denoising,” in *ICASSP*. 2018, pp. 5069–5073, IEEE.
 - [10] Aaron van den Oord, Sander Dieleman, Heiga Zen, Karen Simonyan, Oriol Vinyals, Alex Graves, Nal Kalchbrenner, Andrew Senior, and Koray Kavukcuoglu, “Wavenet: A generative model for raw audio,” 2016, cite arxiv:1609.03499.
 - [11] Daniel Stoller, Sebastian Ewert, and Simon Dixon, “Wave-u-net: A multi-scale neural network for end-to-end audio source separation,” *arXiv preprint arXiv:1806.03185*, 2018.
 - [12] Hakan Erdogan, John R. Hershey, Shinji Watanabe, and Jonathan Le Roux, “Phase-sensitive and recognition-boosted speech separation using deep recurrent neural networks,” in *ICASSP*. 2015, pp. 708–712, IEEE.
 - [13] Donald S. Williamson, Yuxuan Wang, and DeLiang Wang, “Complex ratio masking for monaural speech separation,” *IEEE/ACM Trans. Audio, Speech & Language Processing*, vol. 24, no. 3, pp. 483–492, 2016.
 - [14] Florian Mayer, Donald S Williamson, Pejman Mowlaee, and DeLiang Wang, “Impact of phase estimation on single-channel speech separation based on time-frequency masking,” *The Journal of the Acoustical Society of America*, vol. 141, no. 6, pp. 4668–4679, 2017.
 - [15] G. E. Spoorthi, Subrahmanyam Gorthi, and Rama Krishna Sai Subrahmanyam Gorthi, “Phasenet: A deep convolutional neural network for two-dimensional phase unwrapping,” *IEEE Signal Process. Lett.*, vol. 26, no. 1, pp. 54–58, 2019.
 - [16] Naoya Takahashi and Yuki Mitsufuji, “Multi-scale multi-band densenets for audio source separation,” *CoRR*, vol. abs/1706.09588, 2017.
 - [17] Hyeong-Seok Choi, Jang-Hyun Kim, Jaesung Huh, Adrian Kim, Jung-Woo Ha, and Kyogu Lee, “Phase-aware speech enhancement with deep complex u-net,” *CoRR*, vol. abs/1903.03107, 2019.
 - [18] Shrikant Venkataramani, Jonah Casebeer, and Paris Smaragdis, “End-to-end source separation with adaptive front-ends,” in *2018 52nd Asilomar Conference on Signals, Systems, and Computers*. IEEE, 2018, pp. 684–688.
 - [19] Fabian-Robert Stöter, Antoine Liutkus, and Nobutaka Ito, “The 2018 signal separation evaluation campaign,” in *International Conference on Latent Variable Analysis and Signal Separation*. Springer, 2018, pp. 293–305.
 - [20] Phillip Isola, Jun-Yan Zhu, Tinghui Zhou, and Alexei A. Efros, “Image-to-image translation with conditional adversarial networks,” *2017 IEEE Conference on Computer Vision and Pattern Recognition (CVPR)*, Jul 2017.
 - [21] Fabian-Robert Stöter, Antoine Liutkus, and Nobutaka Ito, “The 2018 signal separation evaluation campaign,” in *Latent Variable Analysis and Signal Separation: 14th International Conference, LVA/ICA 2018, Surrey, UK*, 2018, pp. 293–305.
 - [22] Mark Cartwright, Bryan Pardo, and Gautham J Mysore, “Crowdsourced pairwise-comparison for source separation evaluation,” in *2018 IEEE International Conference on Acoustics, Speech and Signal Processing (ICASSP)*. IEEE, 2018, pp. 606–610.